Nonlinear Lateral Stability of 4-Axle Freight Car with the Y25 Bogies and the Measures to Improve Its Faults

Miroslaw Dusza , Milena Golofit-Stawinska , Krzysztof Zboinski *

Posted Date: 17 April 2024

doi: 10.20944/preprints202404.1140.v1

Keywords: Y25 bogie; numerical model; suspension parameters; stability of motion; vehicle lateral stability

Article

Nonlinear Lateral Stability of 4-Axle Freight Car with the Y25 Bogies and the Measures to Improve Its Faults

Miroslaw Dusza [1], Milena Golofit-Stawinska [2] and Krzysztof Zboinski [3,*]

[1] Warsaw University of Technology, Faculty of Transport; miroslaw.dusza@pw.edu.pl; (M.D.)
[2] Warsaw University of Technology, Faculty of Transport; milena.stawinska@pw.edu.pl; (M.G.)
[3] Warsaw University of Technology, Faculty of Transport; krzysztof.zboinski@pw.edu.pl; (K.Z.)
* Correspondence: krzysztof.zboinski@pw.edu.pl; Tel.: +48 22 234 70 78 (K. Zboinski)

Abstract: The article presents investigations of rail vehicle bogie of Y25 type. The Y25 bogie family is one of the most commonly used freight car bogie designs. In addition to several significant advantages characterising this design, it also has several disadvantages observed since the beginning of more than fifty years of operation in several types of cargo vehicles. One of these defects observed in real systems is "unsatisfactory running stability", particularly at long straight tracks. The article used commercial engineering software VI-Rail to create a model of the gondola car (type 412W Eaos) with two Y25 bogies. The car model was tested empty and loaded (maximum permissible load). Motion along straight and curved tracks with different radii values was analysed. The vehicle velocity was changed from a few m/s to the maximum values for which stable solutions of the model existed. For each route, a non-linear critical velocity was determined, defining the maximum operating velocity of the modelled car. The model solutions were recorded, while just one was selected to present the results - the first wheelset lateral displacement y_{1w}. The opinion about the "imperfect running quality" in curved tracks was confirmed. The possible appearance of self-exciting wheelset vibrations in the modelled car's operating velocity range in the laden state was also observed. The research results on the impact of the bogie suspension parameters change on the vehicle model stability are presented. The crucial parameter in the bogie suspension was indicated. Reducing its value by several percent about the nominal value increases the critical velocity of the car to values higher than the maximum operating velocity of the modelled vehicle.

Keywords: Y25 bogie; numerical model; suspension parameters; stability of motion; vehicle lateral stability

1. Introduction

The research and results discussed in this article are a part of the broader studies on formulation and testing of the novel approach to nonlinear dynamical features of rail vehicles. This approach focuses primarily on velocities around the vehicle's non-linear critical velocity v_n. It comprises all significant conditions of motion, that is, transition curves (TC), circular curves (CC), and straight track (ST). Besides, the TC section is of the higher status in the approach for three reasons: 1 - in terms of track shape geometry, it is a 3-dimensional object, while CCs and ST are 2-dimensional and 1-dimensional objects, respectively; 2 - in terms of place and geometry TC makes the transitional object from ST to CC and vice versa; and 3 - dynamics of vehicles in TC, especially around the v_n, is less researched than dynamics in ST and CC. The draft of the novel approach is described in [1]. The primary tool in the mentioned studies is the numerical simulation of vehicles' dynamics using their numerical models. The studies so far, performed for nine different objects, reveal that all, with no exception, possess strongly non-linear and unexpected features of various nature in the motion conditions of interest. These features make predictions about the objects' behaviour for sure impossible. Results of the studies for six generic objects (three different bogies, two different two-axle freight cars in empty and loaded states, and a four-axle passenger car) are published in part in [2,3]. The subsequent results refer to the second stage of the studies for the existing but no longer produced

 doi:10.20944/preprints202404.1140.v1

three configurations of 4-axle vehicles. These were the passenger car 127A on 25AN bogies, the empty gondola car 412a, and the laden gondola car 412a on Y25 bogies. These results were obtained from the research project mentioned in the Acknowledgements section of this article. The nonlinear critical velocity v_n is the element determined in the novel approach to nonlinear dynamical features of rail vehicles, as vehicle dynamics around this velocity is particularly interesting. Note that v_n is also the main parameter in the nonlinear stability analysis of rail vehicles. Depending on how unfavourable, unexpected, untypical, and faulty the stability features of a given vehicle are, the stability analysis can be a more critical element of the authors' novel approach. So, some minimum makes the v_n determination. Then, we can imagine some more advanced stability studies (for example, for ST only). At the same time, the maximum is a complete stability analysis of the vehicle in ST and CCs of different curve radii R.

Results discussed in this article concern the second stage of the studies, namely for the existing vehicles. More precisely, they represent stability analysis of the gondola car 412a in both empty and laden states. Despite several nonlinear features detected for this freight car, its stability features appeared to be the most important and dominating among all the nonlinear features. Besides, these unfavourable features appeared to refer to the exploitation conditions of this car. Consequently, they needed to be either removed or at least improved. To some extent, the studied gondola car can also represent other freight cars on Y25 bogies. These explain why the results for the 412a car became so important and why the car underwent the complete stability analysis by the authors.

So, the main aim of this article is to present and discuss the stability features of the gondola car on Y25 bogies and the measures undertaken to improve these unfavourable features successfully. The huge volume of the analysis performed justifies gathering stability results of the 412a car into a separate paper without discussing it jointly with other non-linear features of this freight car, all nonlinear features of the 127A passenger car, and conclusions on the novel approach formulation based on the results from the second stage of the studies.

The Y25 bogie series is a conventional European design for freight cars, which has been produced and is widely explored in many countries. Most freight cars, such as container platforms, gondola cars, tank wagons etc., may be equipped with the Y25 type bogies (Figure 1). The main advantages of this bogie design are low cost, low weight, low maintenance and high enough reliability. Despite the unquestionable advantages confirmed by over fifty years of operation, the Y25 bogies' disadvantageous features can also be mentioned. The first to note is imperfect running quality and unsatisfactory running stability [4]. Besides, the poor running performance and history of derailments are also mentioned [5]. In this article, its authors probe into the dynamics of the vehicles with Y25 bogies by results analysis of the vehicle's numerical model. More precisely, relying on previous authors' works [6–8], the lateral stability investigations are executed for the nonlinear rail vehicle-track model.

The additional technical aim of this article can be formulated as to confirm or refute the accusations against the Y25 bogie about its poor running performance. The primary suspension parameters were changed to check the potential for improving bogie behaviour.

Figure 1. This is a figure. Schemes follow the same formatting.

 doi:10.20944/preprints202404.1140.v1

1.1. The Literature Survey

The papers where problems of railway vehicles' stability and determination of nonlinear critical velocity v_n are discussed by present authors are [3,6–8]. A broad reference to the corresponding literature by other authors is provided in these publications, too. The newest example papers on the stability of rail vehicles and their dynamics, also with account taken of motion in CC and TC, are [9–25]. In [9], its authors study the stability of high-speed trains through a focus on bogie behaviour. The novel method of stability determination, based on the root loci methods, is successfully tested. A sensitivity analysis was performed on the selected vehicle parameters, too. In [10], one can see the interesting differences in stability issues for rail and road vehicles. The important influence on the stability of vehicle roll angle is considered. The results for the stability region are presented in a 3-dimensional stability domain. Paper [11] describes a novel measuring system that monitors vehicle hunting motion. The system can predict the wheelset's lateral and yaw displacements and wheel-rail contact relationships in real time based on the monitoring results. The accuracy and efficiency of the whole system were validated by comparing the predicted results with simulated and experimental results. Paper [12] is truly interesting and of high cognitive value. It reveals and verifies experimentally (on a roller rig) the possible existence of parametric vibrations in the wheelset-track system. They appear parallel to self-exciting vibrations (hunting motion) and are caused by wheel load fluctuations. The systems particularly prone to such type of resonance are those with big tread angles. These last also decrease the critical (hunting) velocity, which favours simultaneous existences of self-exciting and parametric vibrations. Publication [13] represents the study of the chaos in a mechanical impacting system. The novelty of this paper lies in the extension of previous results for a 1 degree of freedom (DoF) system on a 2 DoFs system. The existence of phenomena such as narrow band chaos, finger-shaped attractors etc., was demonstrated numerically and then experimentally verified. In [14], the authors propose a new method for stability determination based on the data instead of the equations. With this method, they managed to determine long-term statistics of the chaotic state, the covariant Lyapunov vector, the Lyapunov spectrum, the finite-time Lyapunov exponents, and the angles between the stable, neutral, and unstable splitting of the tangent space. Publication [15] presents and uses one more nonlinear wheelset model to perform bifurcation analysis for him. The nonlinearity in the wheel-rail contact is of primary interest. The analysis comprises comparisons between results for the linearised and nonlinear models. The results for different field-measured wheel profiles are also compared. Finally, the conclusion is that larger suspension stiffness would increase the running stability under wheel wear. Publication [16] is to some extent similar to [15]. The nonlinear wheelset model undergoes the bifurcation analysis. The nonlinear equivalent conicity in wheel-rail contact is of interest. Results for the linear and nonlinear approaches to equivalent conicity and contact forces are compared. The authors show the possible coexistence of stable and unstable limit cycles and expand on the consequences of Chinese high-speed trains' observed unfavourable behaviour. In the paper [17], the authors study the influence of curved track parameters, such as the radius, superelevation, TC and CC lengths, on vehicle-track interactions in the case of side-frame cross-braced 2-axle railway bogie. They conclude that curve radius is of unequivocal importance, TC length is important provided the inflexion point of this importance is not exceeded, superelevation is of minor importance (differences in results for its deficiency and excess are surprisingly small), and CC length is of no importance at all. In [18], the authors focus on vibrations in passenger cars. They compare results from two approaches, one based on analytical solutions of the dynamical equations and the other based on simulation, which means solving the equations numerically. Thanks to the bigger possible DoF's number and smaller simplification of the equations for the simulation approach, the authors conclude that it is superior to the other approach. The authors highlight the higher accuracy of the simulations. Publication [19] compares a few methods of nonlinear critical velocity determination. The simulation approach to this issue and the ramping and path following (continuation) methods are of primary interest. Different methods of hunting motion excitation are compared with each other in terms of the critical velocity value. The influence of the track irregularities (track class) on the results is shown, too, thanks to comparison with the results for an ideal track. In [20], the influence of the bogie suspension parameters on the

 doi:10.20944/preprints202404.1140.v1

track frame lateral forces is studied. The bogie is a three-piece traditional construction applied in freight cars. The authors consider 30 different bolster suspension combinations. It is concluded that increasing the dumping force (the wedge coefficient of friction) increases the lateral frame forces. Simultaneous increases in the lateral stiffness of the bogie and the dumping force increase the lateral frame force, too. On the other hand, the internal interplay between these two parameters appears also important. In [21], the hunting of locomotive carbody is studied experimentally and with simulation. The aim is to explain and suggest measures to eliminate such hunting that appears for low conicity in wheel-rail contact. The measures concern the suspension parameters. Namely, the series stiffness and damping in the yaw damper and the longitudinal stiffness in primary suspension are indicated as those needing the decrease. Both the ST and CC cases have been analysed. In the paper [22], the author studied interactions between vehicle internal elements and between vehicle and track to make sure that existing freight cars with three-piece bogies can run at higher permissible speeds under the increased axle load. The ST and CC sections are considered. It is shown that such increases are possible. However, the bogies have to be replaced with slightly modernised ones. In [23], the authors propose a method to identify, rather than neglect, small amplitude hunting of high-speed railway vehicles. They found that the autocorrelation coefficient and spectral frequency spread are the most efficient parameters for this purpose. The findings are dedicated to supporting the monitoring of hunting instability and the real-time active control studies of high-speed trains. Paper [24] is a general paper on the instability of the limit cycle type oscillations. The aim is to address the need for an efficient computational approach to model instability and handle hundreds or thousands of design variables. It is fulfilled by using a simple metric to determine the stability of the limit cycle utilising a fitted bifurcation diagram slope. The stability derivative of many design variables is efficiently computed with the developed adjoint-based formula. Publication [25] proposes the wheel-rail nonlinear kinematics model, which is an extension of the well-known linear model by Klingel. The nonlinear model comprises high-order odd harmonic frequencies (HOHFs), apart from the fundamental frequency of hunting. Like this last, the HOHFs make the self-exciting vibrations source in rail vehicles. Thus, these findings are important for the methods of hunting instability research and condition monitoring of trains.

Summarising the content of these publications, one can note that their scope is similar to that of the profiled literature from 15 years back. So, we can find the works of cognitive character, the works on new methods of research and description, the works on general dynamics, stability issues, hunting (limit cycles), chaos and so on. Still, the number of works concerning issues for ST is superior to those for CC and TC problems.

1.2. The Fundamental Theoretical Considerations

Although part of the discussed literature directly concerns the stability issue, the fundamentals of the stability phenomenon are given below.

The physical explanation for practical problems of rail vehicle stability is the self-exciting vibrations that appear in vehicle-track systems. They are a phenomenon known for a long time [26]. Some vehicle parts start to undergo self-exciting vibrations at certain motion conditions (parameters). The wheelsets oscillate laterally and around the vertical axis (yawing). The flange wheel-rail contact, noise, and higher risk of derailment accompany them. Although the main vehicle motion along the track is usually possible in such conditions, the self-exciting vibrations make evident adverse phenomena in rail vehicle operation in straight track (ST) and circular curve (CC) sections. The self-exciting vibrations observed in real vehicle-track systems [26] can be identified using the vehicle-track model with bifurcation of its solutions [27,28]. Bifurcation analysis is an effective method to test the modelled object [27–30] and is thus applied also in the presented research. The numerical simulation studies of the vehicle-track system enable us to observe if the model solutions are stable. The stable stationary solutions (constant value of the model's observed coordinate in ST and CC) describe the normal exploitation conditions of a real vehicle. It means that in the real system, each disturbance, for example, caused by track irregularity, is effectively damped while the system tends to equilibrium. The properly designed vehicle should ensure running stability in the expected range

 doi:10.20944/preprints202404.1140.v1

of exploitation parameters changes, such as velocity (0 to v_{max}), load (empty, partially to fully loaded), load asymmetry, track shape (CC, transition curve (TC), ST), track maintenance, etc. The stable stationary solutions of the modelled vehicle-track system in ST and CC are expected for typical operation conditions. In contrast, due to constant change of curve radius and superelevation in TC, stationary solutions in TCs are neither possible nor expected.

The model's stable periodic solutions (limit cycles) are attributed to self-exciting vibrations in the real system. For them, the lateral displacements of a wheelset change periodically during main vehicle motion (along the track). Calling such solutions "stable periodic" is justified because they are limited, observable and can last any length. On the other hand, stable periodic solutions represent the highest abilities of the modelled system in terms of stable behaviour and also bring other valuable information. Nonlinear critical velocity v_n is the key parameter in the stability analysis, and so is the presented research. The v_n value separates the range of vehicle velocity v, where stable stationary solutions exist (v < vn), from the range, where stable periodic solutions may appear ($v \geq v_n$). The v_n value is the minimum vehicle velocity v, at which stable periodic solutions can appear. For a real object, it means self-exciting vibrations may occur, and the vibrational system's state is reached. Further increase of system output (for example, with a rise in v) leads to an increase in the self-exciting vibration amplitude. Finally, amplitude values are not constant anymore, which means unbounded growth of the solutions (loss of stability), which could lead to an accident due to the derailment in the real system. The research of vehicle model periodic solutions for the increased system input (vehicle velocity) in the over-critical system state is interesting. Its conduction is done to reconnoitre how much the system parameters (velocity) can be exceeded to keep the solutions stable (periodic or stationary). A wide range of the system velocity between the value corresponding with periodic solutions' appearance and loss of stability is always desirable for the real vehicle.

2. The Approach to Stability and the Corresponding Model

Part of the studies in the project specified in the Acknowledgements section, which refer to stability analysis, represents, in a general view, the bifurcation approach to stability. Within it, the simulation method of nonlinear lateral stability studies are applied. This method is especially useful when considering rail vehicle systems (vehicles) in their whole dimension. So, when one prefers to consider all the system's degrees of freedom (DoF) rather than one or two degrees of freedom for a single wheelset, The analytical methods can only be applied to such small systems.

On the other hand, the authors used their original approach and method of the lateral stability study in CCs, as elaborated in [6,7]. In this method, the ST case is the case of CC of an infinite curve radius of $R = \infty$. Vehicle velocity v is typically the bifurcation parameter, also here. The authors' original bifurcation diagrams were adopted as a form of results presentation. A couple of diagrams show the maximum of the leading wheelset lateral displacements' absolute value $|y_{lw}|\max$ versus velocity and the peak-to-peak value of the y_{lw} versus velocity. When jointly presenting the couples for all the radii R, one obtains two complex bifurcation diagrams. The authors call such a pair of bifurcation diagrams the stability map [6,7]. The first stability map in this paper is Figure 4, which can serve as an example.

Following the bifurcation approach and their method the authors needed simulation models of the whole vehicle of many DoFs in their studies. Consequently, the rail vehicle model with Y25 bogies was also created and tested. As mentioned before, its first wheelset's lateral displacements y_{lw} were chosen to observe. The whole vehicle-track model was created with the VI-Rail engineering software. This is a discrete model of a type 412W Eaos cargo gondola car (see Figure 2). Bogie models are based on a Y25 construction (also called 25TN in Poland). The car model comprises 15 rigid bodies: a loading platform (gondola), two bogie frames, four wheelsets and eight axle boxes. Rigid bodies are connected with elastic-dumping elements having linear and bi-linear characteristics. Dry friction dampers are applied in the Y25 suspension structure. However, viscous dampers are used in the model to avoid the non-smooth problem with dry friction modelling (stick-slip transition in suspension). In addition, each dry friction damper acts in vertical and lateral directions in the real suspension system. So, to precisely describe the friction forces, a two- dimensional dry friction model

Preprints.org (www.preprints.org) | NOT PEER-REVIEWED | Posted: 17 April 2024 doi:10.20944/preprints202404.1140.v1

should be adopted [31–33]. Two separate viscous dampers in vertical c_{zz} and lateral c_{zy} directions are applied to simplify the bogie model. The sets of vertical coil springs on each axle box are assumed to represent both the vertical k_{zz} and lateral k_{zy} stiffnesses. Each of the parameters mentioned above takes two values. One is for the empty, and the second is for the laden vehicle state (see the Appendix). The wheelset's longitudinal guidance is very stiff. It is a kind of the horn guide [29]. The longitudinal stiffness k_{zx} results from the eventual small deflections of the guide's material. That is why it is also assumed to be independent of the vehicle load.

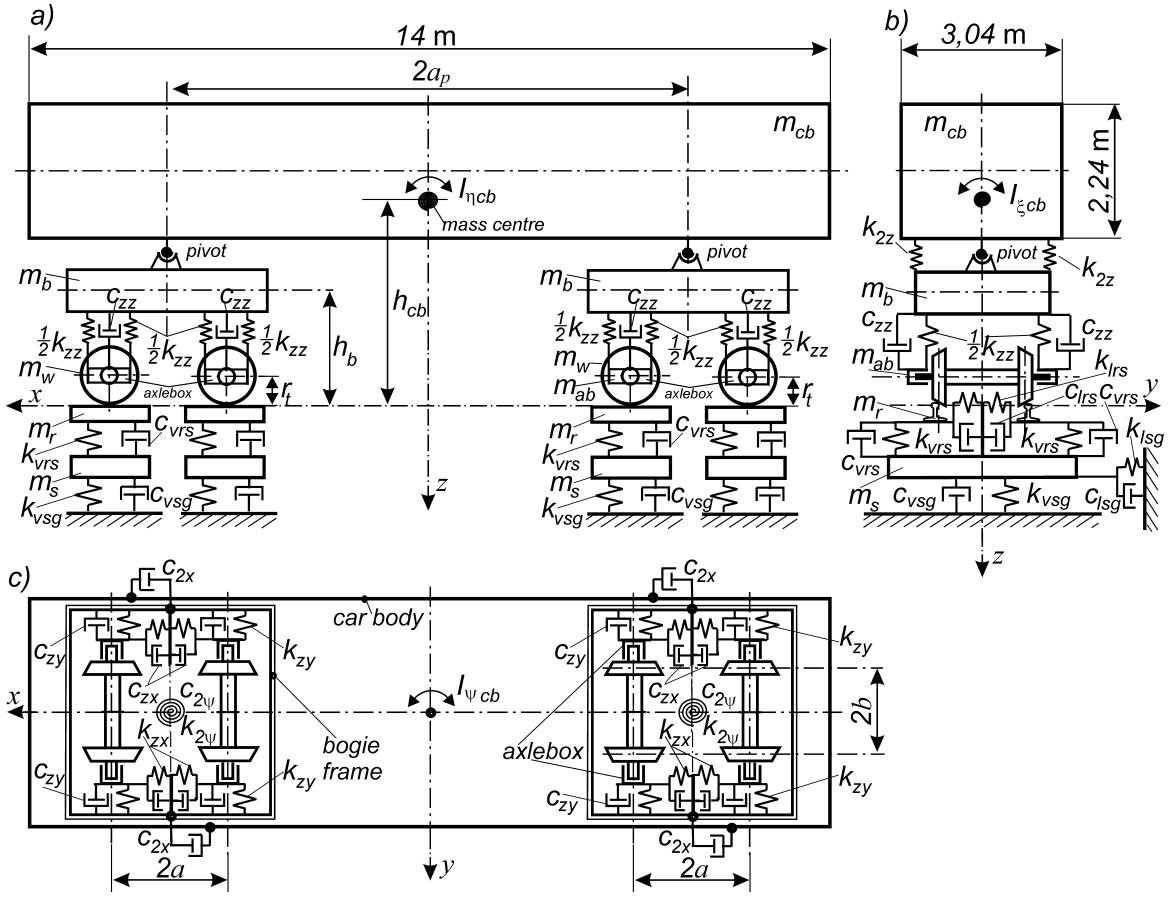

Figure 2. Diagram of the freight vehicle – track system: *a*) side view, *b*) front view, *c*) top view.

A vertically and laterally flexible track model completes the freight car model. Track parameters corresponding to European ballasted track of 1435 mm gauge were adopted. Nominal profiles of S1002 wheels and UIC60 rails with an inclination of 1:40 were used. The non-linear contact parameters are calculated using the ArgeCare RSGEO software. To calculate tangential wheel-rail contact forces, simplified Kalker theory implemented as the FASTSIM procedure is used [34,35]. Equations of motion are integrated with the Gear procedure with step size and error control. It is well suited for solving stiff problems such as the rail vehicle dynamics issue [29,30]. The complete vehicle-track system has 76 kinematic DoFs. Detailed values of the model parameters applied can be found in the Appendix.

3. The Method of Research

The research method consists in the analysis of model solutions for constant vehicle velocity values. The self-exciting vibrations theory is helpful in explaining wheelset oscillations (hunting motion). Vehicle velocity range starts from, e.g. 10 m/s and ends with the maximum value for which the model's stable solutions can be observed. The observed parameter is usually the first wheelset lateral displacement y_{1w} as a function of distance or time. The stable solution term was adopted to describe the model solutions in which y_{1w} has a constant value or periodic value of the limit cycle

Preprints.org (www.preprints.org) | NOT PEER-REVIEWED | Posted: 17 April 2024 doi:10.20944/preprints202404.1140.v1

nature. Such criteria, based on the stable solutions in ST and CC, were also adopted in the analyses presented in this article. Other forms of solution are defined as unstable, although they may meet the other stability criteria, e.g. criteria of technical stability [36].

Figure 3 represents examples of stable solutions typical for vehicle motion velocity lower than critical ($v < v_n$, Figure 3*a*) and higher than critical ($v > v_n$, Figure 3*b*). In this example, the vehicle model motion takes place on a route consisting of sections of ST, TC and CC with a R = 2000 m radius. The wheelset is shifted laterally during TC negotiation and $y_{lw} \neq 0$ in the regular CC section due to track superelevation application. Values of the superelevation in individual CC tracks of different R are collected in Table 1.

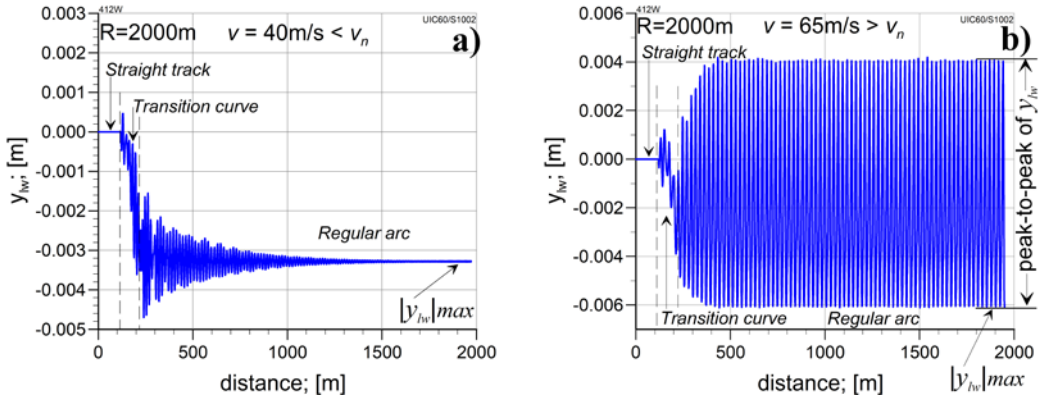

Figure 3. The first wheelset lateral displacements y_{lw} versus distance: (**a**) stable stationary solutions (40 m/s < v_n); (**b**) stable periodic solutions (limit cycle, 65 m/s > v_n).

Table 1. Curve radii tested and track superelevation corresponding to them.

Curve radius; R [m]	1200	2000	3000	4000	6000	∞
Superelevation; h [m]	0.150	0.130	0.110	0.077	0.051	0

It was demonstrated in [7] and in this research that the wheelset's oscillations can be described as a limit cycle of hard excitation. This means that some minimum values of initial conditions are necessary to initiate the vibrations. In the model studies in CCs, the TC negotiation causes the wheelset lateral shift relative to the track, which falls out of equilibrium. This is a way to impose non-zero initial conditions for the solutions in CCs. In the case of analysis in ST, a single lateral irregularity of the track is located 100 m from the track beginning. All wheelsets are shifted laterally, about 0.005 to 0.006 m, due to the negotiation of the irregularity. The first bogie's leading wheelset lateral displacement maximum value $y_{lw}max$ is read from the final section of each simulation diagram. Depending on the track's curve direction and the coordinate systems' adopted orientation, the $y_{lw}max$ may be either positive or negative (as in Figure 3). The negative value corresponds to curves turning to the left-hand side. The solutions for curves turning to the left- and right-hand sides are antisymmetric to each other for the same condition of motion. So, to avoid the sign problem, the maximum absolute value of wheelset lateral displacements $|y_{lw}|max$ is accepted as the result of solutions for a given vehicle velocity. If the solution is stationary (Figure 3*a*), $|y_{lw}|max$ is the only solution value. If the solution is periodic (Figure 3*b*), peak-to-peak values of y_{lw} are also read off and recorded. Peak-to-peak of y_{lw} = 0 for the stationary solutions. Thus, $|y_{lw}|max$ and peak-to-peak value of y_{lw} are read from each simulation of motion performed for a constant velocity v and radius R and finally presented as a stability map. As already said, the stability map is a pair of diagrams showing $|y_{lw}|max$ and peak-to-peak of y_{lw} (p-t-p of y_{lw} in short) as a function of vehicle velocity for CCs of different radii R (the example in Figure 4). The diagrams enable us to observe the nature of the solutions, values of the solutions, and value of the critical velocity v_n in the range of velocity v for which stable solutions exist. When stationary solutions exist only, particularly in the v range below the critical value v_n, the presentation of results starts from v slightly below the v_n value (30 m/s in this research usually) and covers the over-critical velocity range. Each line on the diagrams refers to a

Preprints.org (www.preprints.org) | NOT PEER-REVIEWED | Posted: 17 April 2024 doi:10.20944/preprints202404.1140.v1

specific route, CC of track of a constant radius R (marked with different line colour). The last point of each line corresponds to the highest velocity for which a stable solution (stationary or periodic) was obtained. The authors' detailed examples of stability determination can be found in [6–8,37].

4. Results of the Research

4.1. The Empty Car Analysis

The stability maps for the motion of the empty wagon model are shown in Figure 4. As can be seen there, the properties of the model are regular. That is, for each of the tested routes the critical velocities v_n were determined. Just stable stationary solutions appear for velocities lower than the critical ones. The periodic solutions exist for velocities equal to and greater than the critical values v_n. The values of critical velocity v_n on each curved track increase with the curve radius decrease (Table 2). The smallest value is 37.2 m/s for an ST ($R = \infty$), and the highest v_n is 45.2 m/s for a CC with a R = 1200 m radius. Stable periodic solutions still exist at velocities greater than 200 m/s in the ST (black line). The velocity ranges where periodic solutions in CCs occur are smaller than in ST and decrease as the curve radius decreases (different line colours for particular R values). For each CC section and the final range of velocities, there is a bifurcation of periodic to stationary solutions, which are the stable ones. Potentially, it could be the effect of a centrifugal force action. Only stable stationary solutions exist in the range of velocities lower than the critical value, with $|y_{lw}|$max values increasing according to the curve radius decrease. Therefore, the diagrams show results for motion velocity higher than 30 m/s. The lack of wheelsets' central location in CCs below v_n ($|y_{lw}|\max \neq 0$) results from motion conditions, including the applied track superelevation (Table 1).

So, in light of the tests carried out on the car model in an empty state, the requirements regarding motion stability for operating velocities (less than 120 km/h ≈ 33.33 m/s) are met. The critical velocities on particular tested routes are not lower than the maximum operational velocity. The periodic solutions with $|y_{lw}|$max values up to approximately 0.006 to 0.007 m appear for the critical- and bigger than critical velocities. This means that the wheelsets' self-exciting vibrations may occur in the modelled system. Still, the basic vehicle motion (along the track) is possible in the over-critical velocity range, too.

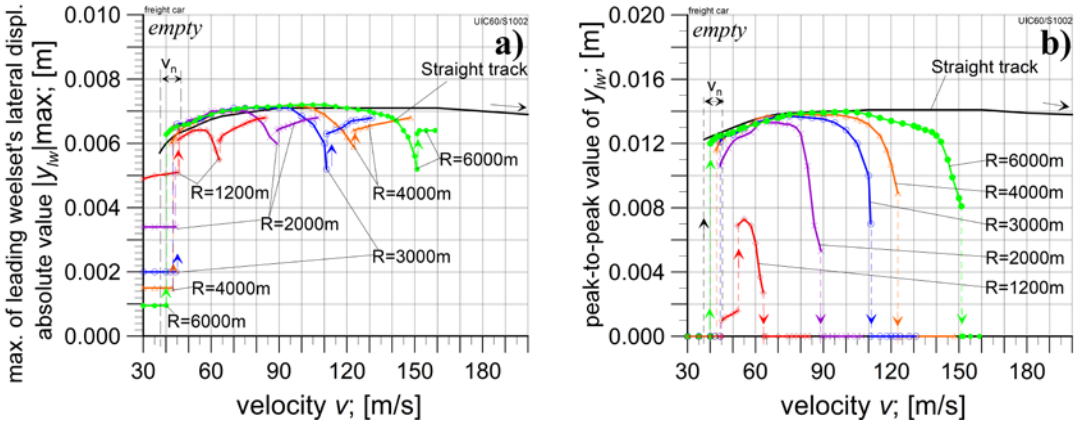

Figure 4. Empty car stability map: (**a**) maximum of leading wheelset's lateral displacements absolute value $|y_{lw}|max$ and; (**b**) peak-to-peak value of y_{lw} versus vehicle velocity.

Table 2. The modelled vehicle critical velocity values v_n.

Curve radius R [m]		**1200**	**2000**	**3000**	**4000**	**6000**	**∞**
Empty;	**v_n [m/s]**	45.2	44.4	44.4	42.6	40.1	37.2
Loaded;	**v_n [m/s]**	55.8	43.7	33	45.6	45	30.8

Preprints.org (www.preprints.org) | NOT PEER-REVIEWED | Posted: 17 April 2024 doi:10.20944/preprints202404.1140.v1

4.2. The Loaded Car Analysis

The laden vehicle model presents significantly different features in the same motion conditions (track curvatures, Figure 5) as compared to the empty one. The lowest value of the critical velocity occurs on an ST, where v_n = 30.8 m/s. It is lower than the maximum vehicle operating velocity, i.e. 120 km/h ≈ 33.3 m/s. This means self-exciting vibrations may appear in the modelled car during regular operation. Critical velocities are higher in CCs (Table 2) than in ST. In the range of overcritical velocities, there exist bifurcations of solutions: from periodic to stationary and from stationary to periodic on an ST and CC of the R = 6000 m radius. These make the stability maps hardly legible. Therefore, the analysis of selected solutions on the routes for the loaded car is presented in separate diagrams further on.

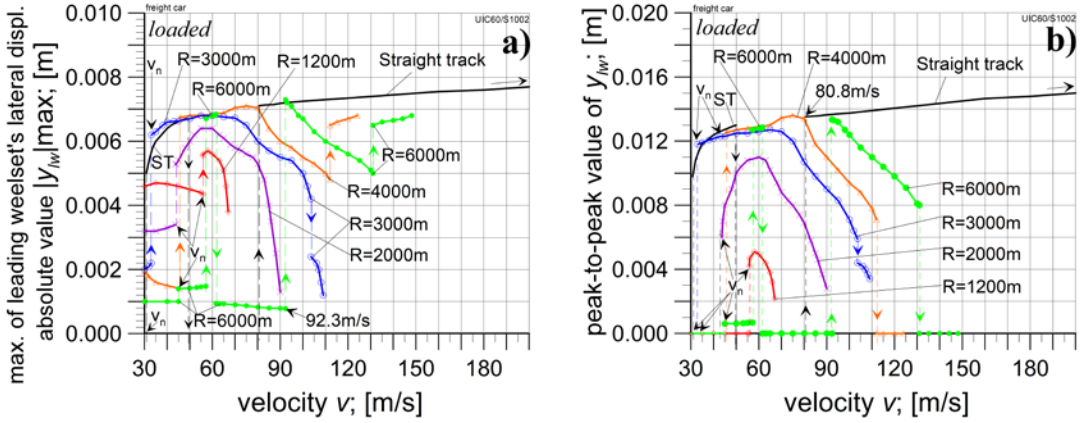

Figure 5. Loaded car stability map: (**a**) maximum of leading wheelset's lateral displacements absolute value $|y_{lw}|max$ and; (**b**) peak-to-peak value of y_{lw} versus vehicle velocity.

4.2.1. The Analysis in Straight Track

Periodic solutions that appeared on the ST at 30.8 m/s exist until velocity v equals 49.9 m/s (Figure 6). Increasing the v over this value by 0.1 m/s causes the bifurcation of periodic solutions to stationary ones. The stationary solution persists up to the v of 80.7 m/s. Increasing the velocity v by 0.1 m/s further causes the bifurcation to a periodic solution again. The periodic solutions last to the end of the tested velocity range (200 m/s).

Next, the research was undertaken to eliminate the possibility of the periodic solutions occurrence (self-exciting vibrations in real systems) in the modelled car operating velocity range. Elements of the suspension system have a crucial impact on the dynamic properties of the vehicle. Change of suspension parameter values is usually a relatively simple process. Thus, the influence of the primary suspension stiffness and damping in the longitudinal (k_{zx}, c_{zx}) and lateral (k_{zy}, c_{zy}) directions was examined using their value variation. The result of these tests is the determination of lateral stiffness k_{zy} parameter as that whose reduction in relation to the nominal value gives the most favourable effects, i.e. the betterment in the analysed car properties. The test results are shown in Figure 7.

Reducing the lateral stiffness to 90% of the nominal value (90% ·k_{zy} = 0.9·55.6·10^5 ≈ 50·10^5 [N/m]), increases the critical velocity to 36.9 m/s. At this velocity, periodic solutions appear and exist up to 45.3 m/s. Then, bifurcation from periodic to stationary solution appears. Stationary solutions exist for velocity increased up to 112.5 m/s. Subsequent increases in velocity v cause the bifurcation from the stationary to the periodic solution with values close to those obtained for the nominal value of k_{zy}. Periodic solutions persist up to velocities exceeding 200 m/s. Further decrease in the lateral stiffness value, down to 80% of the nominal value (80% · k_{zy} = 0.8·55.6·10^5 ≈ 44.5·10^5 [N/m]), causes a jump of the critical velocity value. In this case, the range of periodic solutions, which existed at velocities lower than 50 m/s, disappears. The stationary solutions exist for velocity being increased up to 136.1 m/s. Then, bifurcation to periodic solution occurs. Values of solutions are similar to those obtained for the nominal value of the lateral stiffness. Such solutions exist up to the velocity of 200 m/s. So, a

Preprints.org (www.preprints.org) | NOT PEER-REVIEWED | Posted: 17 April 2024 doi:10.20944/preprints202404.1140.v1

decrease of lateral stiffness k_{zy} by a dozen percent relative to the nominal k_{zy} value enables the improvement of stability properties of the loaded car in the ST.

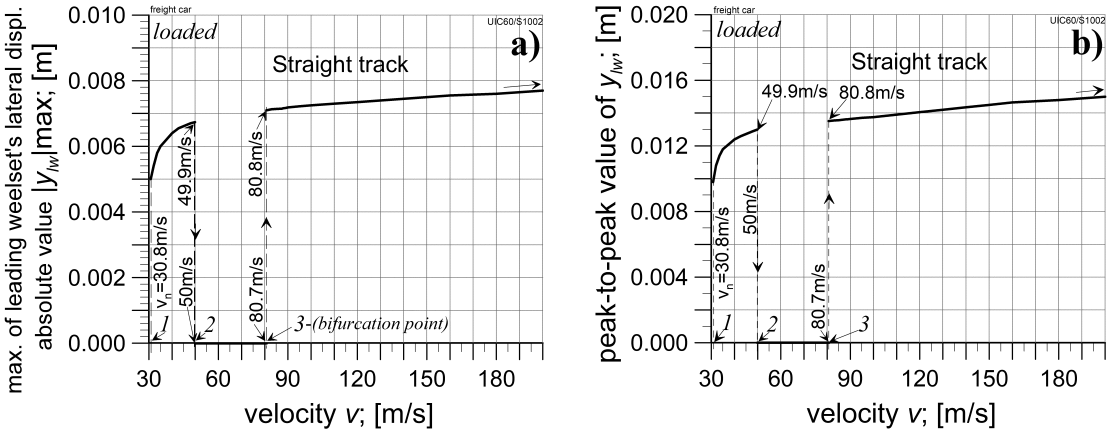

Figure 6. Loaded car stability map in an ST. The nominal value of lateral stiffness applied k_{zy} = 55.6*10^5 N/m.: (**a**) maximum of leading wheelset's lateral displacements absolute value $|y_{lw}|max$ and; (**b**) peak-to-peak value of y_{lw} versus vehicle velocity.

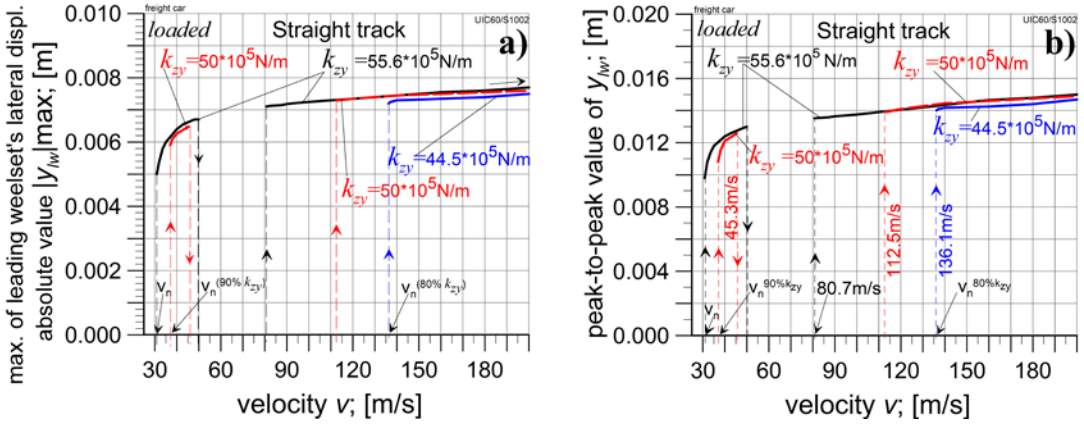

Figure 7. The lateral stiffness k_{zy} influence on laden car first wheelset. k_{zy} = 55.6*10^5 N/m – nominal value (black line), k_{zy} = 50*10^5 N/m – 90% of nominal value (red line), k_{zy} = 44.5*10^5 N/m – 80% of nominal value (blue line). Motion in the ST: (a) maximum lateral displacements absolute value and; (b) peak-to-peak of wheelset lateral displacements.

4.2.1. The Analysis in Curved Tracks

The following research step examined whether the beneficial effect for an ST (regarding the betterment in system properties) due to reducing the lateral stiffness k_{zy} would also appear with its favourable improvement in the CC of R = 6000 m radius. For the nominal value k_{zy} = 55.6·10^5 N/m, the agreed critical velocity was v_n = 45 m/s (Figure 8). It was decided to some extent arbitrary because at lower v (about 20 m/s), "periodic" solutions of the very small p-t-p value of y_{lw} appeared. Velocity v_n = 45 m/s was adopted, judging that the p-t-p of y_{lw} are large enough (about 0.001 m) at this velocity to talk about periodic solutions in the practical sense. However, a considerable increase in the p-t-p value of y_{lw} to a dozen millimetres is observed at the velocity of 57.1 m/s. The stable periodic solutions exist up to the v = 61.6 m/s only, replaced by the bifurcation to the stationary solution. For further increasing velocity, the stationary solutions exist up to 92.3 m/s. Then, bifurcation to the stable periodic solution is observed. Periodic solutions exist until v = 131 m/s. Next, the bifurcation to a stable stationary solution appears. Such solutions exist for high velocity range from 131 to 148 m/s. For even bigger velocities, no stable solutions are observed.

In the next research step, the lateral stiffness was reduced to 90% of the nominal value k_{zy} = 0.9·55.6·10^5 ≈ 50·10^5 N/m. Stable stationary solutions exist up to a velocity of 102 m/s. Although,

 doi:10.20944/preprints202404.1140.v1

similarly to the model with nominal value of lateral stiffness, some "periodic" lateral displacements of the wheelset appear on the curve too, but they have very small peak-to-peak values. An increase of vehicle velocity to 102.1 m/s results in bifurcation to periodic solutions. Such solutions exist for velocity increased up to 131 m/s.

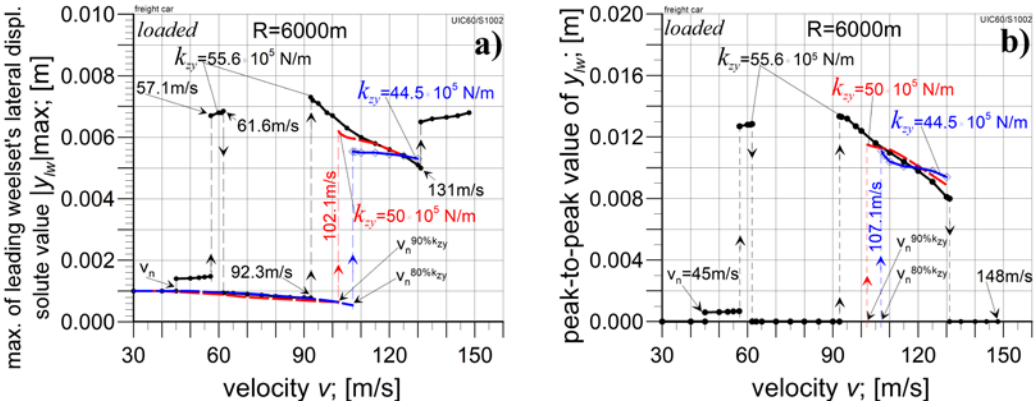

Figure 8. The lateral stiffness k_{zy} influence on laden car first wheelset. k_{zy} = 55.6*10⁵ N/m – nominal value (black line), k_{zy} = 50*10⁵ N/m – 90% of nominal value (red line), k_{zy} = 44.5*10⁵ N/m – 80% of nominal value (blue line). Motion in CC of radius R = 6000 m: (a) maximum lateral displacements absolute value and; (b) peak-to-peak of wheelset lateral displacements.

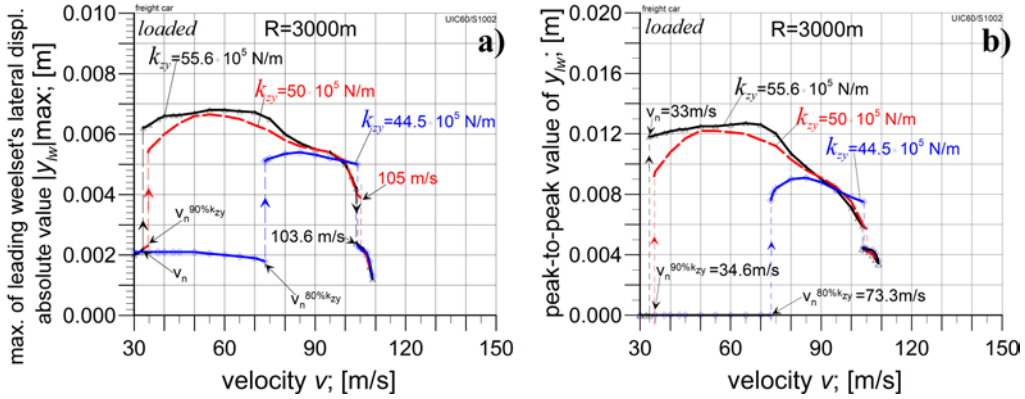

Figure 9. The lateral stiffness k_{zy} influence on laden car first wheelset. k_{zy} = 55.6*10⁵ N/m – nominal value (black line), k_{zy} = 50*10⁵ N/m – 90% of nominal value (red line), k_{zy} = 44.5*10⁵ N/m – 80% of nominal value (blue line). Motion in the CC of radius R = 3000 m: (a) maximum lateral displacements absolute value and; (b) peak-to-peak value of wheelset lateral displacements.

The lateral stiffness was reduced to 80% of the nominal value (80% · k_{zy} = 0.8·55.6·10⁵ ≈ 44.5·10⁵ [N/m]) in the next step. Stable stationary solutions exist up to the velocity of 107.1 m/s. At this velocity, the bifurcation of solution from stable stationary to stable periodic occurs. Periodic solutions persist up to a velocity of about 130 m/s. Values of solutions ($|y_{lw}|$ max and p-t-p of y_{lw}) for each tested k_{zy} value are similar. Thus, reducing the lateral stiffness by several percent in relation to the nominal k_{zy} value causes a significant increase in the critical velocity on the curved track with a radius of R = 6000m.

The critical velocity v_n = 33 m/s for the nominal k_{zy} value in motion along a CC with a radius R = 3000 m. So, it is slightly lower than the car's maximum operating velocity (120 km/h ≈ 33.3 m/s). Stable periodic solutions persist up to the velocity of 103.6 m/s in this case. Next, bifurcation to also periodic solutions but of a smaller p-t-p value (approx. 0.004 m) appears. A velocity of 109 m/s is the maximum value at which the stable solution occurs. Reducing the lateral stiffness to 90% of the nominal value (50·10⁵ N/m) increases the critical velocity to v_n = 34.6 m/s. Periodic solutions persist up to the velocity of 105 m/s, after which they bifurcate to periodic solutions with smaller p-t-p value (approx. 0.004

 doi:10.20944/preprints202404.1140.v1

m). The maximum velocity for which solutions were still stable was 108 m/s. In the next step, the lateral stiffness was reduced to 80% of the nominal value ($44.5 \cdot 10^5$ N/m). As a result, there was an abrupt increase in the critical velocity to v_n = 73.3 m/s. Periodic solutions exist up to the velocity of 104 m/s, after which they bifurcate to also periodic solutions with smaller p-t-p values. Velocity 109 m/s was the highest value, for which the solutions were still stable. Summing up this stage of research, it can be stated that reducing the lateral stiffness in the vehicle's primary suspension by several percent in relation to the nominal stiffness value brings beneficial effects in the vehicle's motion along the straight as well as curved track. To supplement the studies of the k_{zy} influence on vehicle model's solutions stability, it should be checked how reducing k_{zy} will affect the tested car model properties when it is empty.

4.3. The Empty Car Analysis for Reduced k_{zy} Value

A moderate effect of reducing the lateral stiffness in the primary suspension can be observed in motion along an ST (Figure 10). The critical velocity v_n decreases from 37.2 m/s for nominal k_{zy} value ($38.9 \cdot 10^5$ N/m), to 36.5 m/s for 90% · $k_{zy} \approx 35 \cdot 10^5$ N/m, and to 35.8 m/s for 80% · $k_{zy} \approx 31 \cdot 10^5$ N/m. So, the v_n is greater than the required minimum v_n = 33.3 m/s. The nature of the model solutions is analogous for each k_{zy} value. That is, for velocities lower than v_n, there are stationary solutions only, and for velocities greater than v_n, there are periodic solutions that persist up to velocities greater than 200 m/s. The values of the solutions are similar for each value of k_{zy}.

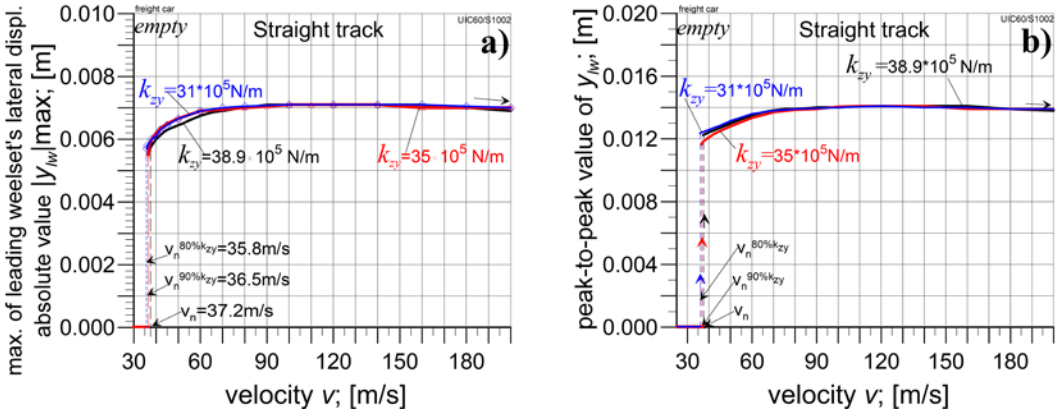

Figure 10. The lateral stiffness k_{zy} influence on empty car first wheelset. $k_{zy} = 38.9 \cdot 10^5$ N/m – nominal value (black line), $k_{zy} = 35 \cdot 10^5$ N/m ≅ 90% of nominal value (red line), $k_{zy} = 31 \cdot 10^5$ N/m ≅ 80% of nominal value (blue line). Motion in the ST: (a) maximum lateral displacements absolute value and; (b) peak-to-peak of wheelset lateral displacements.

The influence of the k_{zy} on the investigated model parameters is also moderate in the case of motion in curved tracks. The critical velocity is 40.1 m/s for the nominal k_{zy} value and large radius curve of R = 6000 m (Figure 11). Reducing the lateral stiffness causes a slight decrease in the critical velocity to the values v_n = 39.6 m/s for 90% k_{zy} and v_n = 39.2 m/s for 80% k_{zy}, respectively. Stable periodic solutions persist for increased velocity up to about 151 m/s, followed by bifurcation to stationary solutions. Stable stationary solutions exist up to the velocity of about 176 m/s. The model solution values for particular k_{zy} applied, are similar in the entire velocity range.

The critical velocity is 44.4 m/s on a CC with a smaller R = 3000 m radius, for the nominal value of k_{zy} = $38.9 \cdot 10^5$ N/m (Figure 12). Reducing the lateral stiffness to 90% k_{zy}decreased the critical velocity to 44.2 m/s. Further reduction of the lateral stiffness to 80% k_{zy} reduced the critical velocity to 44 m/s only. So, a moderate influence of the k_{zy} decrease on the critical velocity on this route is also observed. Values of the model solutions ($|y_{lw}|$ max and p-t-p of y_{lw}) for individual k_{zy} are similar to values on the previously studied routes. Thus, it can be observed that reducing k_{zy} to 80% of the nominal value reduces the model's critical velocity in the empty state, but not more than by 1 m/s.

Preprints.org (www.preprints.org) | NOT PEER-REVIEWED | Posted: 17 April 2024 doi:10.20944/preprints202404.1140.v1

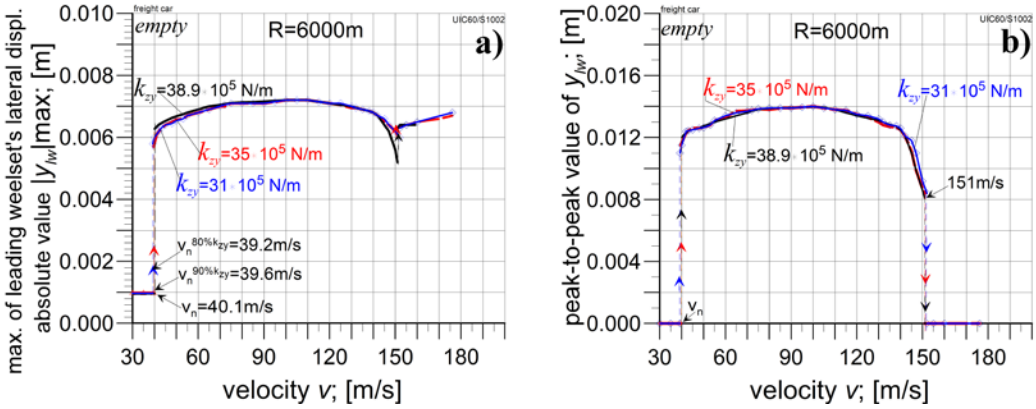

Figure 11. The lateral stiffness k_{zy} influence on empty car first wheelset. k_{zy} = 38.9*10^5 N/m – nominal value (black line), k_{zy} = 35*10^5 N/m ≅ 90% of nominal value (red line), k_{zy} = 31*10^5 N/m ≅ 80% of nominal value (blue line). Motion in the CC of radius R = 6000 m: (a) maximum lateral displacements absolute value and; (b) peak-to-peak of wheelset lateral displacements.

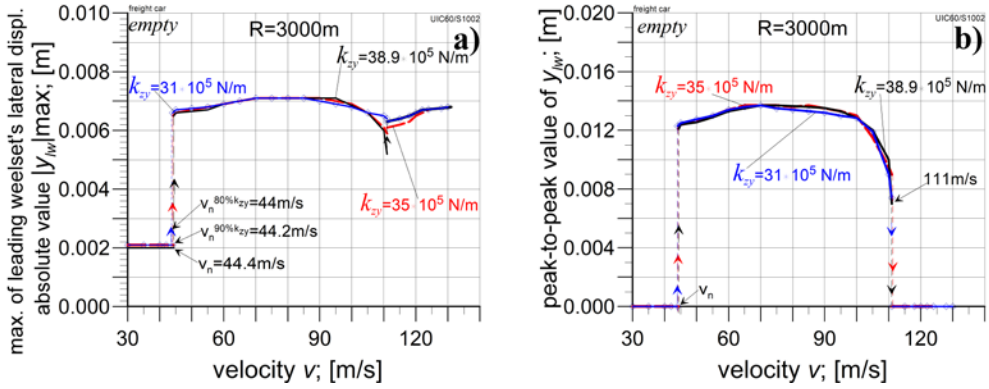

Figure 12. The lateral stiffness k_{zy} influence on the first wheelset of an empty car. k_{zy} = 38.9*10^5 N/m – nominal value (black line), k_{zy} = 35*10^5 N/m ≅ 90% of nominal value (red line), k_{zy} = 31*10^5 N/m ≅ 80% of nominal value (blue line). Motion in the CC of radius R = 3000 m: (a) maximum lateral displacements absolute value and; (b) peak-to-peak of wheelset lateral displacements.

5. Conclusions

A thorough scan of the 412W gondola car exploited in Poland (also by Polish State Railways) for nonlinear features revealed the existence of several such features. On the other hand, the only unfavourable nonlinear features closely related to the car's real conditions of exploitation were the stability features. It appeared that unfavourable features of such type concern the studied gondola car in the fully loaded state. The same vehicle in an empty state possesses satisfactory stability properties for the real conditions of its exploitation. The stability map in Figure 4, for the empty car, represents uniform character for all curve radii R, including ST (R = ∞). Most importantly, the nonlinear critical velocities v_n for all these R are above the maximum admissible exploitation velocity v_{ad} equal to 33.3 m/s (120 km/h). The smallest v_n = 37.2 m/s exists for ST. This means that the empty car avoids (is protected against) hunting motion, which is desirable for sure. In the case of the stability map for the fully loaded gondola in Figure 5, the stability features are not as uniform as for the empty gondola. One can see the uniform solutions starting from R = 3000 m and going down to R = 1200 m. For the ST and R = 6000 m, additional, untypical, and to some extent unfavourable bifurcations of solutions from stable periodic to stable stationary exist above the critical velocities v_n. Moreover, the v_n for R = ∞, 6000, and 3000 m is smaller or relatively close to the maximum admissible exploitation velocity v_{ad}. The v_n equals 30.8, 45.5, and 33.0 m/s, respectively. So formally, the ST and R = 3000 m cases appeared to need correction from the viewpoint of the exploitation velocities. And so it happened, the corresponding measures were found successfully.

 doi:10.20944/preprints202404.1140.v1

The analysis of the freight car in the type of a gondola with the Y25 type bogies shows that it has the potential to improve the motion properties through minor corrections of the suspension parameter values. From the point of view of the tested vehicle model properties, it is possible to increase the car's critical velocity in the laden state by reducing the lateral stiffness in primary suspension k_{zy} by several or a dozen percent relative to the nominal value. The k_{zy} reduced to 80% of its nominal value is indicated as recommended by the authors. In addition to the bigger critical velocity value in ST (v_n = 136.1 m/s), the critical velocities in CC increased favourably for all R, too. They are v_n = 107.1 and 103.6 m/s for R = 6000 and 3000 m, respectively. Besides, the reduction of k_{zy} causes the disappearance of periodic solutions of very small peak-to-peak values on CCs. This could mean an improvement in the curved track negotiation of the real gondola car of the studied type. One should notice that reducing k_{zy} to just 90% of its nominal value could also be counted as a successful measure to improve the gondola's nonlinear features. Then, v_n for ST, R = 6000 m, and R = 3000 m equal 36.9, 102.1, and 34.6 m/s, respectively. All of them are bigger than 33.3 m/s. On the other hand, two of them are quite close to v_{ad}. In particular, the value for R = 3000 m resulted in a safety margin that was too small. One should also remember here that the accuracy of v_n determination is limited.

An important element of the study's result and an important fact, at the same time, is that the measure found for the loaded gondola car does not spoil the results for the empty car. Figures 10–12 for the empty vehicle show that for R = ∞, 6000, and 3000 m the decrease of k_{zy} stiffness to 90 and 80% of its nominal value changes critical velocities v_n insignificantly. Although such a decrease also decreases v_n, which is unfavourable, the changes obtained are negligible. The most significant change happened in Figure 10 for ST, and it was the change of v_n from 37.2 to 35.8 m/s. It can be seen that 35.8 is still enough higher than v_{ad} = 33.3 m/s.

Finally, it should be noted that the results obtained apply only to the particular tested type of car. For other types of freight cars using Y25 bogies, the observed effects need individual studies, and only then can their eventual confirmations be shown.

Funding: This work is a result of the research project financed by the National Center for Research and Development, Poland, under the TANGO program – project no. TANGO-IV-A/0027/2019-00.

Author Contributions: Conceptualization, K.Z.; methodology, KZ and M.D.; software, K.Z. and M.D.; validation, KZ., M.D. and M.G.; formal analysis, K.Z..; investigation, M.D., M.G. and K.Z.; resources, M.G. and M.D.; data curation, M.D.; writing—original draft preparation, M.D. and K.Z.; writing—review and editing, K.Z.; visualization, M.D and M.G..; supervision, K.Z.; project administration, K.Z.; funding acquisition, K.Z. and M.G. All authors have read and agreed to the published version of the manuscript.

Institutional Review Board Statement: Not applicable.

Conflicts of Interest: The authors declare no conflicts of interest.

Appendix A

Table A1. Parameters of the freight car accepted to research.

Notation	Description	Unit	Value	
			empty	loaded
m_{cb}	Vehicle body mass	kg	11 000	72 000
m_b	Bogie frame mass	kg	1 600	
m_w	Wheelset mass	kg	1 400	
m_{ab}	Axlebox mass	kg	100	
$I_{\circledcirc cb}$	Body moment inertia; longitudinal axis	kg·m²	17 300	90 055
$I_{\circledcirc cb}$	Body moment inertia; lateral axis	kg·m²	188 500	1 210 606
$I_{\circledcirc cb}$	Body moment inertia; vertical axis	kg·m²	188 140	1 231 450
$I_{\circledcirc b}$	Bogie frame inertia moment; longitudinal axis	kg·m²	790	

 doi:10.20944/preprints202404.1140.v1

$I_{\varnothing b}$	Bogie frame inertia moment; lateral axis	kg·m²	1 000	
$I_{\varnothing b}$	Bogie frame inertia moment; vertical axis	kg·m²	1 090	
$I_{\varnothing w}$	Wheelset inertia moment; longitudinal axis	kg·m²	747	
$I_{\varnothing w}$	Wheelset inertia moment; lateral axis	kg·m²	131	
$I_{\varnothing w}$	Wheelset inertia moment; vertical axis	kg·m²	747	
k_{zz}	Vertical stiffness of the primary suspension	kN/m	1 017	2 280
k_{zy}	Lateral stiffness of the primary suspension	kN/m	3 890	5 560
k_{zx}	Longitudinal stiffness of the primary suspension	kN/m	12 000	12 000
c_{zz}	Vertical damping of the primary suspension	kN·s/m	7	123.3
c_{zy}	Lateral damping of the primary suspension	kN·s/m	42	138
c_{zx}	Longitudinal damping of the primary suspension	kN·s/m	100	
k_{2z}	Vertical stiffness of the bogie frame – car body side bearer	kN/m	22 500	
c_{2x}	Longitudinal damping on the bogie frame – car body side bearer	kN·s/m	6	10
$k_{2\varnothing}$	Torsional stiffness between bogie frame and car body	kN·m/rad	20	
$c_{2\varnothing}$	Torsional damping between bogie frame and car body	kN·m·s/rad	0.5	
a_p	Half of bogie's pivot-pivot distance	m	4.5	
a	Semi-wheel base	m	0.9	
tc	Semi-tape circle distance	m	0.75	
h_b	Vertical distance between bogie frame centre mass and track plane	m	0.69	
h_{cb}	Vertical distance between car body centre mass and track plane	m	1.5	1.87
r_t	Wheel rolling radius	m	0.46	

References

1. Zboinski, K.; Golofit-Stawinska, M. Dynamics of a Rail Vehicle in Transition Curve above Critical Velocity with Focus on Hunting Motion Considering the Review of History of the Stability Studies. Energies 2024, 17, 967. https://doi.org/10.3390/ en17040967.
2. Zboinski, K.; Golofit-Stawinska, M. Investigation into nonlinear phenomena for various railway vehicles in transition curves at velocities close to critical one. Nonlinear Dyn. 2019, 98, 1555–1601. https://doi.org/10.1007/s11071-019-05041-2.
3. Zboinski, K.; Golofit-Stawinska, M. Determination and Comparative Analysis of Critical Velocity for Five Objects of Railway Vehicle Class. Sustainability 2022, 14, 6649. https://doi.org/10.3390/ su14116649.
4. Csiba, J. Bogie type anniversary: the bogie type Y25 is over 50 years. Proceedings of the 10th International Conference On Railway Bogies And Running Gears, Budapest, 12-15 September, 2016, 253-262.
5. Pagaimo, J.; Magalheas, H.; Costa, J.N.; Ambrosio, J. Derailment study of railway cargo vehicle using a response surface methodology. Vehicle System Dynamics 60(1), 309-334, 2022.
6. Zboiński, K.; Dusza, M. Self-exciting vibrations and Hopf's bifurcation in non-linear stability analysis of rail vehicles in curved track. European Journal of Mechanics - Part A/Solids, 29(2), 190–203, 2010.
7. Zboiński, K.; Dusza, M. Extended study of rail vehicle lateral stability in a curved track. Vehicle System Dynamics 49(5), 789–810, 2011.
8. Zboiński, K.; Dusza, M. Bifurcation analysis of 4-axle rail vehicle models in a curved track. Nonlinear Dynamics 89(2), 863–885, 2017, ISSN 0924-090X, https://doi.org/10. 1007/s11071-017-3489-y.
9. Bustos, A.; Tomas-Rodriguez, M.; Rubio, H.; Castejon, C. On the nonlinear hunting stability of a high-speed train boogie, Nonlinear Dynamics, 111, 2059–2078, 2023, https://doi.org/10.1007/s11071-022-07937-y.
10. Xiao, F.; Hu, J.; Zhu, P. *et al.* A method of three-dimensional stability region and ideal roll angle to improve vehicle stability. Nonlinear Dynamics 111, 2353–2377, 2023, https://doi.org/10.1007/s11071-022-07965-8.
11. Sun, J.; Meli, E.; Song, X.; Chi, M.; Jiao, W.; Jiang, Y. A novel measuring system for high-speed railway vehicles hunting monitoring able to predict wheelset motion and wheel/rail contact characteristics, Vehicle System Dynamics, 61(6), 1621-1643, 2023, DOI: 10.1080/00423114.2022.2086145.

12. Umemoto, J.; Yabuno H. Parametric and self-excited oscillation produced in railway wheelset due to mass imbalance and large wheel tread angle, Nonlinear Dynamics, 111:4087–4106, 2023, https://doi.org/10.1007/s11071-022-08056-4.
13. Seth, S., Kudra, G., Wasilewski, G. *et al.* Study the bifurcations of a 2DoF mechanical impacting system. Nonlinear Dynamics 112, 1713–1728, 2024, https://doi.org/10.1007/ s11071 -023-09119-w.
14. Margazoglou, G.; Magri, L. Stability analysis of chaotic systems from data. Nonlinear Dynamics 111, 8799–8819, 2023, https://doi.org/10.1007/s11071-023-08285-1.
15. Guo J.; Shi H.; Luo R.; Zeng J. Bifurcation analysis of a railway wheelset with nonlinear wheel–rail contact, Nonlinear Dynamics, 104, 989–1005, 2021, https://doi.org/10.1007/s11071-021-06373-8.
16. Ge P.; Wie X.; Liu J.; Cao H. Bifurcation of a modified railway wheelset model with nonlinear equivalent conicity and wheel-rail force, Nonlinear Dynamics, 102, 79–100, 2020, https://doi.org/10.1007/s11071-020-05588-5.
17. Yang, C.; Huang, Y.; Li, F. Influence of Curve Geometric Parameters on Dynamic Interactions of Side-Frame Cross-Braced Bogie. Proceedings ICRT 2021, Second International Conference on Rail Transportation, ASCE Library 2022.
18. Chernysheva, Y.; Gorskiy, A. Methods Proposed for Analysis of Vibrations of Railway Cars. In: Manakov, A.,Edigarian, A. (eds) International Scientific Siberian Transport Forum TransSiberia - 2021. TransSiberia 2021. Lecture Notes in Networks and Systems, vol 402. Springer, Cham., 2022, https://doi.org/10.1007/978-3-030-96380-4_46.
19. Skerman, D.; Colin Cole, C.; Spiryagin, M. (2022) Determining the critical speed for hunting of three-piece freight bogies: practice versus simulation approaches, Vehicle System Dynamics, 60(10), 3314-3335, DOI: 10.1080/00423114.2021.1944648.
20. Pandey M., B. Bhattacharya B.; Effect of bolster suspension parameters of three-piece freight bogie on the lateral frame force, International Journal of Rail Transportation, 8(1), 45-65, 2020, DOI: 10.1080/23248378.2019.1593059.
21. Sun J.; Chi M.; Jin X.; Liang S.; Wang J.; Li W. (2021) Experimental and numerical study on carbody hunting of electric locomotive induced by low wheel–rail contact conicity, Vehicle System Dynamics, 59(2), 203-223, 2021, DOI: 10.1080/00423114.2019.1674344.
22. Shvets A.O.: Dynamic interaction of a freight car body and a three-piece bogie during axle load increase, Vehicle System Dynamics, 60(10), 3291-3313, 2022, DOI: 10.1080/00423114.2021.1942930.
23. Guo J.; Zhang G.; Shi, H.; Zeng J. Small amplitude bogie hunting identification method for high-speed trains based on machine learning, Vehicle System Dynamics, Published online 19 Jun 2023, DOI: 10.1080/00423114.2023.2224906.
24. He, S.;E. Jonsson, E.; Martins, J.R.R.A. Adjoint-based limit cycle oscillation instability sensitivity and suppression. Nonlinear Dynamics 111, 3191–3205, 2023, https://doi.org/10.1007/s11071-022-07989-0.
25. Wang, X.; Lu, Z.; Wen, J.; Wie, J.; Wang, Z. Kinematics modelling and numerical investigation on the hunting oscillation of wheel-rail nonlinear geometric contact system, Nonlinear Dynamics 107, 2075–2097, 2022, https://doi.org/10.1007/s11071-021-07103-w.
26. Knothe, K.; Böhm, F. History of Stability of Railway and Road Vehicles. Vehicle System Dynamics 31, 283-323,1999.
27. Kass-Petersen, C.; True H. A bifurcation analysis of nonlinear oscillations in railway vehicles. Vehicle System Dynamics 13, 655-665, 1984.
28. True, H. On the theory of nonlinear dynamics and its applications in vehicle systems dynamics. Vehicle System Dynamics 31, 393-421, 1999.
29. Iwnicki, S. (ed.). Handbook of railway vehicle dynamics. CRC Press Inc. 2006.
30. Shabana, A. A.; Zaazaa, K. E.; Sugiyama, H. Railroad Vehicle Dynamics: A Computatio-nal Approach. 2008, Taylor & Francis LLC and the CRC.
31. Piotrowski, J.; Pazdzierniak, P.; Adamczewski, T. Curving dynamics of freight wagon with one- and two-dimensional friction damping. Proc. Of the 10th Mini Conference on Vehicle System Dynamics, Identification and Anomalies. Ed. Zobory I. Budapest 6-8 November 2006, 215-222.
32. Bruni, S.; Vinolas, J.; Berg, M.; Polach, O.; Stichel, S. Modeling of suspension components in a rail vehicle dynamics context. Vehicle System Dynamics 49(7), 1021-1072, 2011.
33. Evans, J.; Berg, M. Challenges in simulation of rail vehicle dynamics. Vehicle System Dynamics 47(8), 1023-1048, 2009.
34. Kalker, J. J. A fast algorithm for the simplified theory of rolling contact. Vehicle System Dynamics 11, 1-13, 1982.
35. Piotrowski, J. Kalker's algorithm Fastsim solves tangential contact problems with slip-dependent friction and friction anisotropy. Vehicle System Dynamics 48(7), 869-889, 2010.
36. Bogusz, W. Technical stability (in Polish *Stateczność techniczna*). PWN, 1972, Warsaw.

 doi:10.20944/preprints202404.1140.v1

37. Dusza, M. Rail vehicle model possibility of safe motion analysis in the overcritical velocity range. Proceedings of the 11th International Conference on Railway Bogies and Running Gears, Ed. Istvan Zobory, Department of Rolling Stock, SSME/GTE, ISBN 978-963-9058-42-2, Budapest, 2020, 159-168.